inter·noise 2009
innovations in practical noise control
2009 August 23-26
Ottawa, Canada

Imaging of the atmosphere with infrasound

Läslo G. Evers[a]
Seismology Division
Royal Netherlands Meteorological Institute
Wilhelminalaan 10, 3732 GK De Bilt, the Netherlands

Acoustic Remote Sensing
DEOS, Faculty of Aerospace Engineering, Delft University of Technology
Kluyverweg 1, 2629 HS Delft, the Netherlands

ABSTRACT

Ground-truth sources in infrasound are rare but very useful for assessing the accuracy of wind and temperature models for propagation and the propagation itself. In this study, seismic and infrasound signals are used from explosions in Finland observed at the seismic array ARCES in Norway between 2001 and 2006. The seismic signals deliver the ground-truth in terms of origin time and location. The variability in the infrasound signals is caused by the atmosphere as the seismic signals are almost similar throughout the years. Conventional modeling only partly explains the observations. A hypothesis is tested that partly reflections due to fine scale structure in the stratosphere cause arrivals on the edge of the shadow zone. Such phases are not covered by the models.

1. INTRODUCTION

Infrasound is applied as a monitoring technique for the Comprehensive Nuclear-Test-Ban Treaty (CTBT). Currently, a world-wide network of 60 infrasound arrays is being installed to monitor the atmosphere for nuclear tests as part of the International Monitoring System (IMS)[1]. The IMS also comprises seismic stations for underground tests, hydro-acoustic stations for underwater explosions and radionuclide measurements as additional atmospheric monitoring technique. The application of two monitoring techniques for the atmosphere reflects the complexity of the medium. Temporal and spatial variations in the wind and temperature structure make the atmosphere a dynamic medium. Infrasound serves as relatively fast sensing technique with respect to radionuclide propagation which is much slower in detecting but gives direct evidence. Ground truth infrasonic events are rare, most events lack accurate information on the origin time or location or both. Accidental or human-made explosions are among the few sources that often have accurate ground truth information, this information can also be derived with other techniques like seismics in so-called seismo-acoustic analysis[2,3]. Some ground truth may also be available from natural sources. Examples of sources with some ground truth on location or time are earthquakes[4,5], chemical explosions[6], mine blasts[7] and volcanoes[8]. Studies with ground truth sources are essential for successfully applying infrasound as monitoring techniques since detection algorithms and phase identifiers can be tested and atmospheric propagation models can be validated. Furthermore, the accuracy of location procedures can be assessed.

[a] Email address: evers@knmi.nl

2. OBSERVATIONS OF EXPLOSIONS

A dataset of seismic and infrasound recordings from the destruction of old ammunition was recently presented[9], spanning six years of observations. The associated explosions take place in Finland and are observed by seismometers in Finland and Norway. Measurements are conducted by single stations of three component seismometers in Finland (KEV, IVL and SGF) and an array of seismometers in Norway (ARC). These stations are shown in Figure 1.

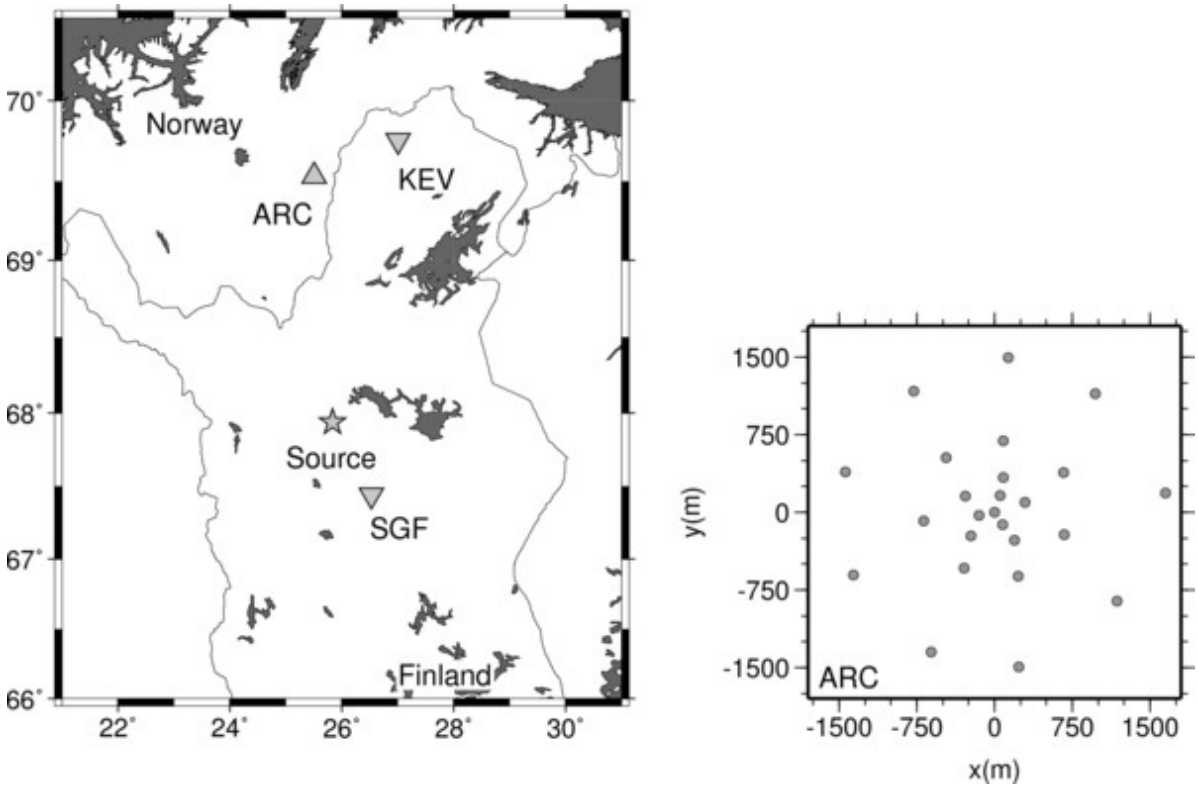

Figure 1: The location of the source, where old ammunition is destroyed, and seismometers (KEV, IVL and SGF) in Finland and the seismic array ARC in Norway. The layout of ARC is given in a separate figure.

Seismic signals of the explosions are analyzed to obtain the origin time and the location, providing the ground truth. Infrasound arrivals are observed between roughly 500 to 700 s after the seismic P and S phases. The occurrence of the infrasound arrivals strongly varies with time as do the number of arrivals, the arrival times and amplitudes. The seismic signals are almost identical as function of time, indicating that the variability in the infrasound recordings is caused by the dynamical atmosphere.

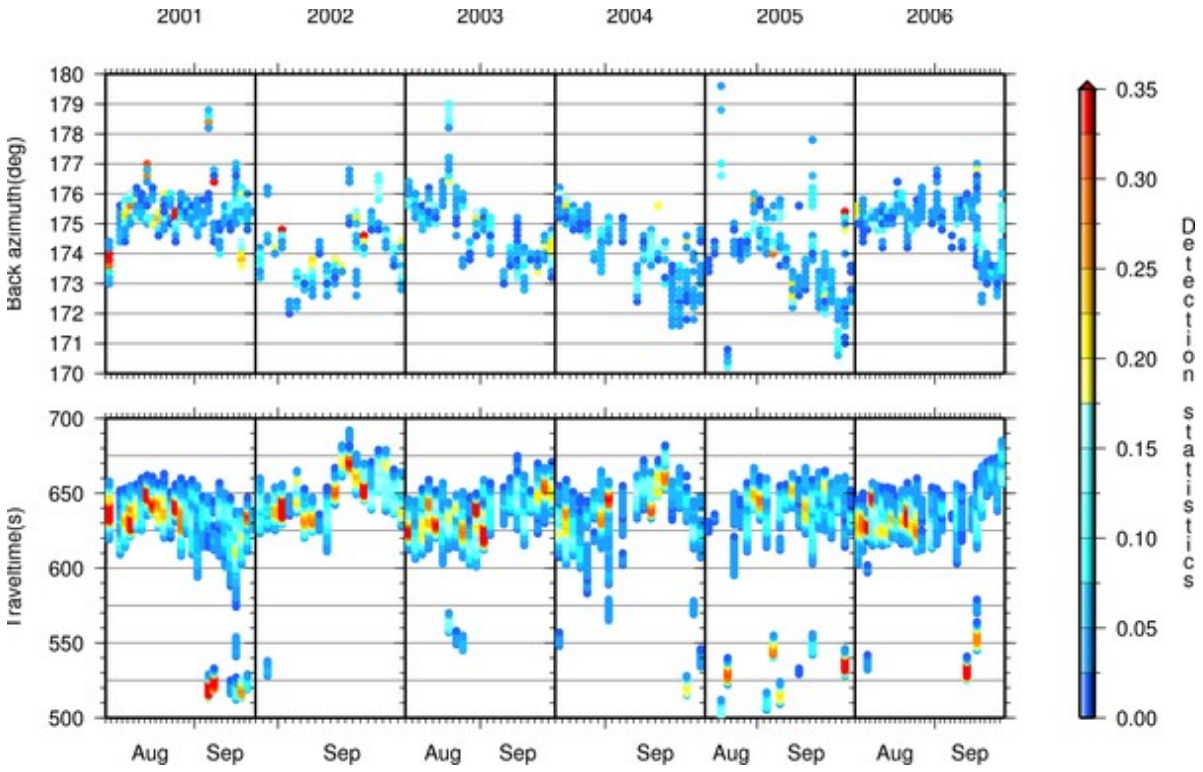

Figure 2: Observations and results from array processing of the infrasound recorded at ARC. Six year of results are shown, from 2001 to 2006, where the explosions occurred during August and September. Traveltimes from source to receiver are shown in the lower frame. The upper frame gives the observed back azimuths as follow from array processing. Color coded is the detection statistic which is a measure of signal coherency. The most coherent arrivals occur as red dots.

Figure 2 shows the variety of observed traveltimes and back azimuths from the infrasound of the explosions recorded at ARC. The results of six years of data are given, where the explosions occurred in August and September. The observed traveltimes are a function of the wind and temperature along the propagation paths. The back azimuths are furthermore influenced by cross winds acting on the wavefront. The aim of this paper is to understand the infrasound recordings at ARC in Norway from the destruction of old ammunition in Finland. Furthermore, atmospheric models can be validated and, if necessary, adjusted based on this ground truth dataset and propagation modeling tools like raytracing and normal modes.

3. PROPAGATION CHARACTERISTICS

The propagation of infrasound is, in first order, dependent on the wind and temperature structure of the atmosphere. The effective sound speed (v_{eff}) for an infrasonic wave is proportional to the square root of the temperature and the wind along the source-receiver trajectory[10]. In a standard atmosphere, infrasound from a surface explosion is bend upwards due to the decrease in temperature with height. Refractions of infrasound back to the surface may occur in regions where v_{eff} becomes larger than its surface value which will direct the energy downwards to the earth's surface. Refractions can be caused by an increase in wind or temperature or due to a combination of both effects. Two regions control long range sound propagation, i.e. propagation over distances larger than several hundreds of kilometers, that are the stratosphere and thermosphere.The source-receiver distance between the ammunition destruction site and ARC is

179 km, making also tropospheric propagation feasible. The troposphere is the region where the daily weather takes place and variations occur on all possible temporal and spatial scales. The tropopause between 10 and 15 km altitude is an area of constant temperature and marks the boundary between the troposphere and stratosphere. Infrasonic phases traveling in the troposphere are labeled as *Iw* and come in various forms. Refractions may occur from the jet stream, a strong wind at the top of the troposphere, near the bottom tropopause, at roughly 10 km altitude. This wind is zonally symmetric and westerly which means that its motion is from the west. Planetary waves, finding their origin in near e.g. mountains, may displace the circumpolar flow out of zonal symmetry. Furthermore, synoptic weather systems distort the circulation into a wavy pattern that meanders around the globe. These unsteady disturbances deflect the general air stream meridionally and migrate from west to east[11]. Synoptic weather systems can also, partly or fully, deflect the jet stream. Lower level jets may also increase the v_{eff} to higher values that its surface value, an example of such a wind is the nocturnal jet. Other strong winds can either facilitate or counteract infrasound propagation and are related to synoptic weather systems. In a standard atmosphere, the temperature decreases with height, a temperature increase with height is called a temperature inversion and can efficiently trap acoustic energy. Infrasound may also directly travel from the source to the receiver through the troposphere without refractions. The temperature in the stratosphere reaches its maximum value of roughly 0 deg C around 50 km altitude due the absorption of solar radiation by ozone. Furthermore, strong winds due to the polar vortex may occur at these altitudes up to values 150 m/s. This combined wind and temperature effect results in high values of v_{eff} and subsequently refraction of infrasound. Phases turning at these altitudes and arriving at a ground-based receiver are abbreviated as *Is*. Multiple bounces can occur between the earth's surface and top of the stratospheric duct, phases are than labeled *Is2*, *Is3*, etc. The polar vortex changes direction twice a year making the observation of *Is* phases seasonally dependent. The vortex is directed eastwards in the northern hemisphere winter[12]. After a decrease in temperature within the mesosphere, the temperature increases again in the thermosphere from 100 km altitude and upwards which is caused by the direct impact of solar radiation on the particles. Phases returning from these altitudes are abbreviated with *It*. Although *It* phases are always predicted, they may not always be observed due to the high attenuation in the strongly rarefied upper atmosphere[13]. *It* phases are not considered in this study because the observed traveltimes are too small to allow for these long propagation paths. To exemplify some of the above features, two specific cases will be addressed in the next chapter, illustrating the propagation characteristics between the source and ARC.

4. TROPOSPHERIC AND STRATOSPHERIC ARRIVALS AT ARC

A. Two types of tropospheric arrivals on 2005, August 27

Figure 3 shows an atmospheric model valid for 2005, August 27 12h UT at 25.5E, 68.5N which is halfway the source and ARC. The model is obtained from the European Centre for Medium-Range Weather Forecasts (ECMWF, http://www.ecmwf.int). The temperature, in the left frame of Figure 3, decreases with altitude in the troposphere up to the tropopause where it reaches a constant value around 10 km altitude. An increase in temperature is visible in the stratosphere, owing to the ozone layer, up to a maximum of 0 deg C in the stratopause around 50 km altitude. The temperature then decreases again in the mesosphere until it reaches the mesopause and subsequently the thermosphere where an increase will occur from 100 km and upwards.

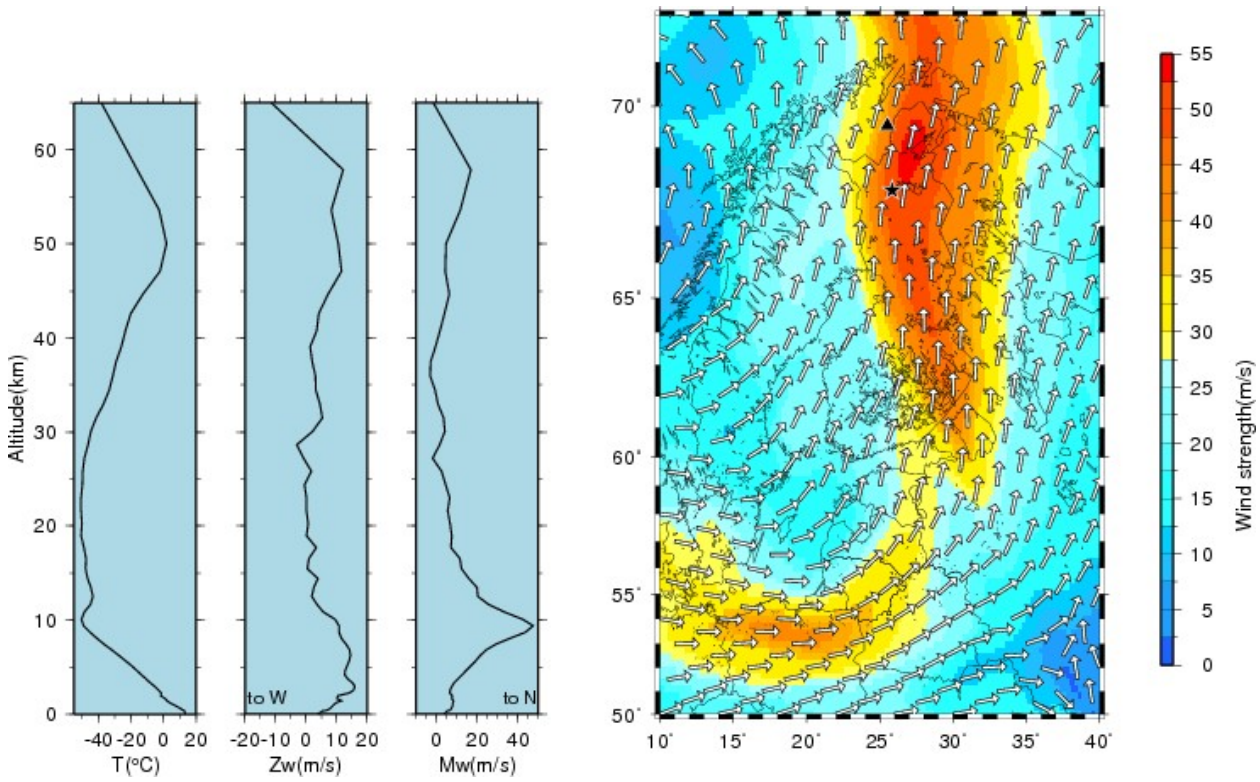

Figure 3: Wind, temperature and effective sound speed profiles for 2005, August 27 12 UT at 25.5E, 68.5N. The wind is split in a zonal or west-east (Zw) and meridional or south-north (*Mw*) component, having a positive sign when blowing to the east and north, respectively. The wind field at an altitude of 10 km where the vectors indicate the wind direction and the colors represent the wind strength in m/s, is given in the right hand frame. The air stream is bend from a west-east direction to a south-north direction at higher latitudes.

The zonal wind does not show much variability as function of altitude, although, the sign and strength of the zonal wind often, globally, determines the detectability of infrasound. This profile is around the time of the year that the zonal wind changes from being easterly to a westerly, reducing the strength of the polar vortex around 50 km altitude to almost zero. The meridional wind shows a strong increase in strength around 10 km and is blowing towards the north. The source and ARC are on a south-north bearing (see Figure 1), therefore, this wind will increase the effective sound speed as can be seen in the right frame of Figure 3. The dashed vertical line is the surface sound speed and the strong meridional helps to increase v_{eff} to a large value around 10 km altitude. Turning rays will occur from this altitude since v_{eff} is larger than its surface value.Another significant increase in wind, and consequently v_{eff} , is also present around 500 m altitude. The strong wind around 10 km height is caused by a low pressure system located above the Atlantic Ocean, in between Norway, Greenland and Iceland. This synoptic system causes a south to north air stream over Sweden and Norway, having its maximum close to the source-ARC path, see Figure 3. Although, the jet stream will be seriously deflected by such systems, this wind at 10 km altitude should be considered as part of the low pressure system.

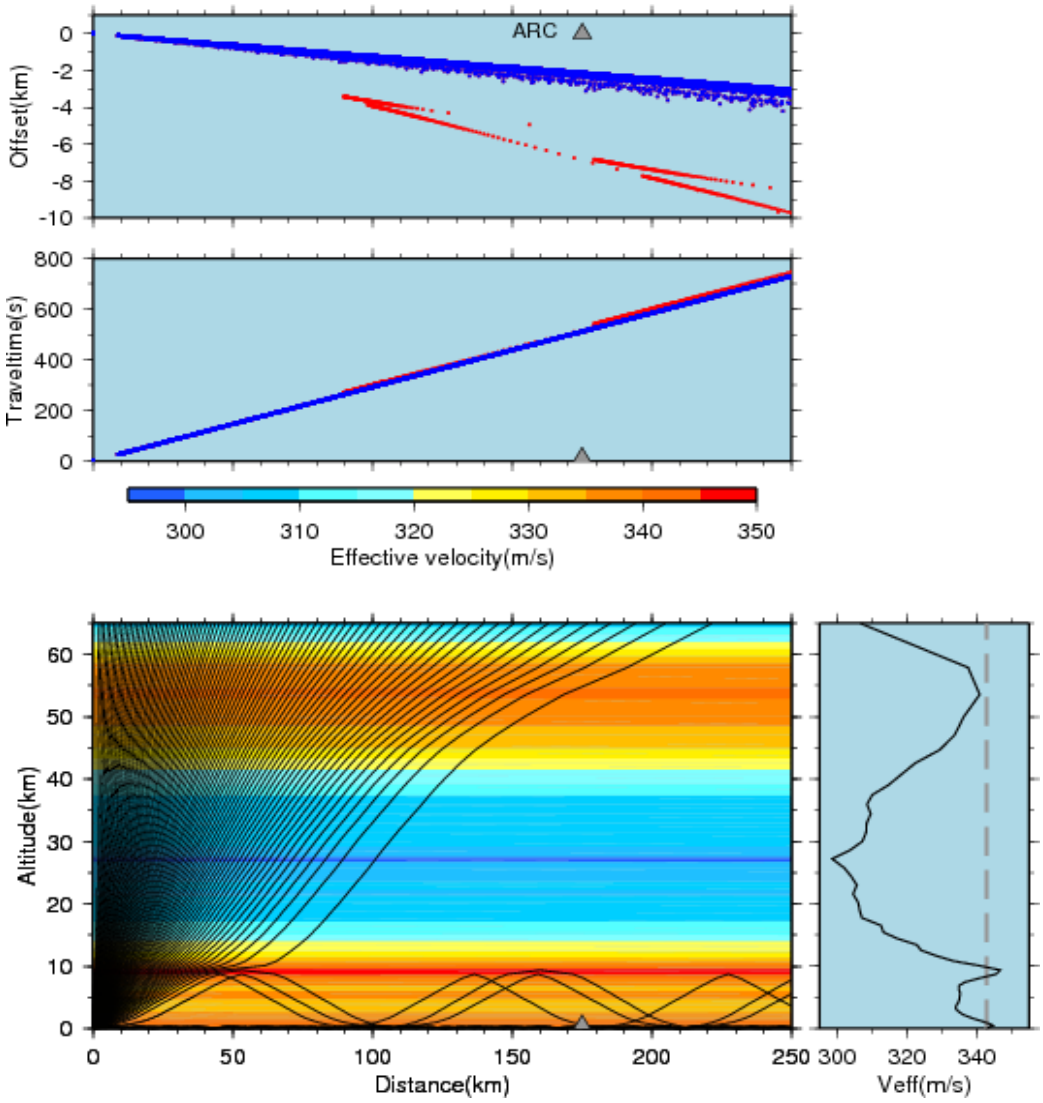

Figure 4: Raytracing results through the effective sound speed profile for energy leaving the source in the direction of ARC. The lower frame shows the ray trajectories indicating a duct around 500 m and 9 km. Traveltimes are plotted in the middle frame, black is used for arrivals in the 500 m duct and gray for rays trapped near the tropopause. The same color convention is used in the top frame, where the amount of offset is plotted for rays being shot in the direction from the source to ARC.

Raytracing through the effective sound speed model reveals the different phases and their propagation characteristics[14], see Figure 4. The lower frame shows the ray trajectories where the energy is trapped in either the 500 m or 9 km duct. Rays leaving the source at small launch angles, with respect to the vertical, might be reflected from the thermosphere or escape the atmosphere, i.e. for very small launch angles. Thermospheric refractions are not considered in this study based on the observed traveltimes and source-receiver distance which are too small. Raytracing through climatological models (HWM/MSISE[15]) has revealed that the first thermospheric returns occur on average at a distance of 265 km of the source after having traveled for 1200 s. The middle frame of Figure 4 gives the traveltimes of the different phases, black is used for the 500 m duct and gray for 9 km duct. The traveltime difference between the two arrivals is small in the first bounce range of the 9 km phases, between 80 and 120 km

distance. A somewhat larger difference is modeled for the second bounce range of 18 s (523 s for the 500 m and 541 s for the 9 km duct). Offsets are plotted in the top frame. An offset is the location where a ray impinges the surface when shot from the source to ARC. Cross winds will deviate the wavefront which results in an azimuthal deviation being the difference between the true and observed back azimuth. The wind in both ducts has a north-eastern direction this means that the rays are deviated to the east of ARC resulting in a negative sign for both offsets. Azimuthal deviations can be derived from Figure 4 by taking the tangent of the offset and source-receiver distance. Doing so, a value of -0.7 and -2.3 deg is obtained for, respectively, the 500 m and 9 km duct. Modeling of the propagation on 2005, August 27 indicates the arrival of at least two phases with a significant traveltime difference and a large difference in azimuthal deviations. Amplitude variations should also be observed in the data caused by the difference in refraction height. The phase from 9 km altitude has only experienced one bounce while the 500 m phase has bounced many times in a thin near-surface turbulent layer. Therefore, the phase from 9 km altitude should be relatively undisturbed with respect to the phases caught in the 500 m duct.

B. Stratospheric arrivals on 2004, September 07

The same approach as taken in the previous section is applied in this section to illustrate arrivals from the stratosphere, which are labeled as *Is*. Figure 5 shows temperature and wind profiles for 2004, September 07. The profiles are again valid for the location halfway the source and receiver at 12 UT.

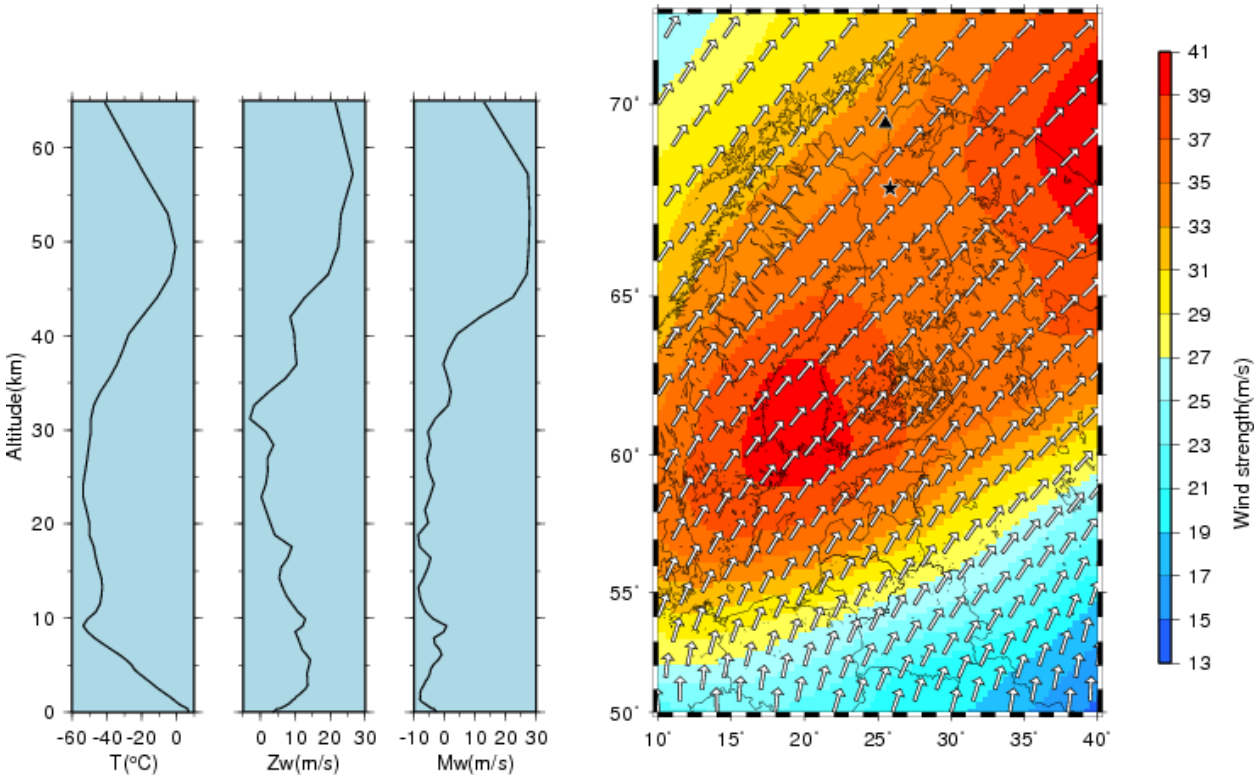

Figure 5: Wind, temperature and effective sound speed profiles for 2004, September 07 12 UT at 25.5E, 68.5N. The wind field at an altitude of 50 km where the vectors indicate the wind direction and the colors represent the wind strength in m/s, see right hand frame.

Both the zonal and meridional wind have gained strength in the stratosphere, when compared to

the values in Figure 3. The positive signs indicate a wind directed to the northeast which is along the propagation path of the infrasound. This is resembled in the right hand frame of Figure 6 as an increase of v_{eff} in the stratosphere from approximately 35 km and upwards. The wind field at an altitude of 50 km is shown in Figure 5. Such a wind field should be regarded as a snapshot of the polar vortex.

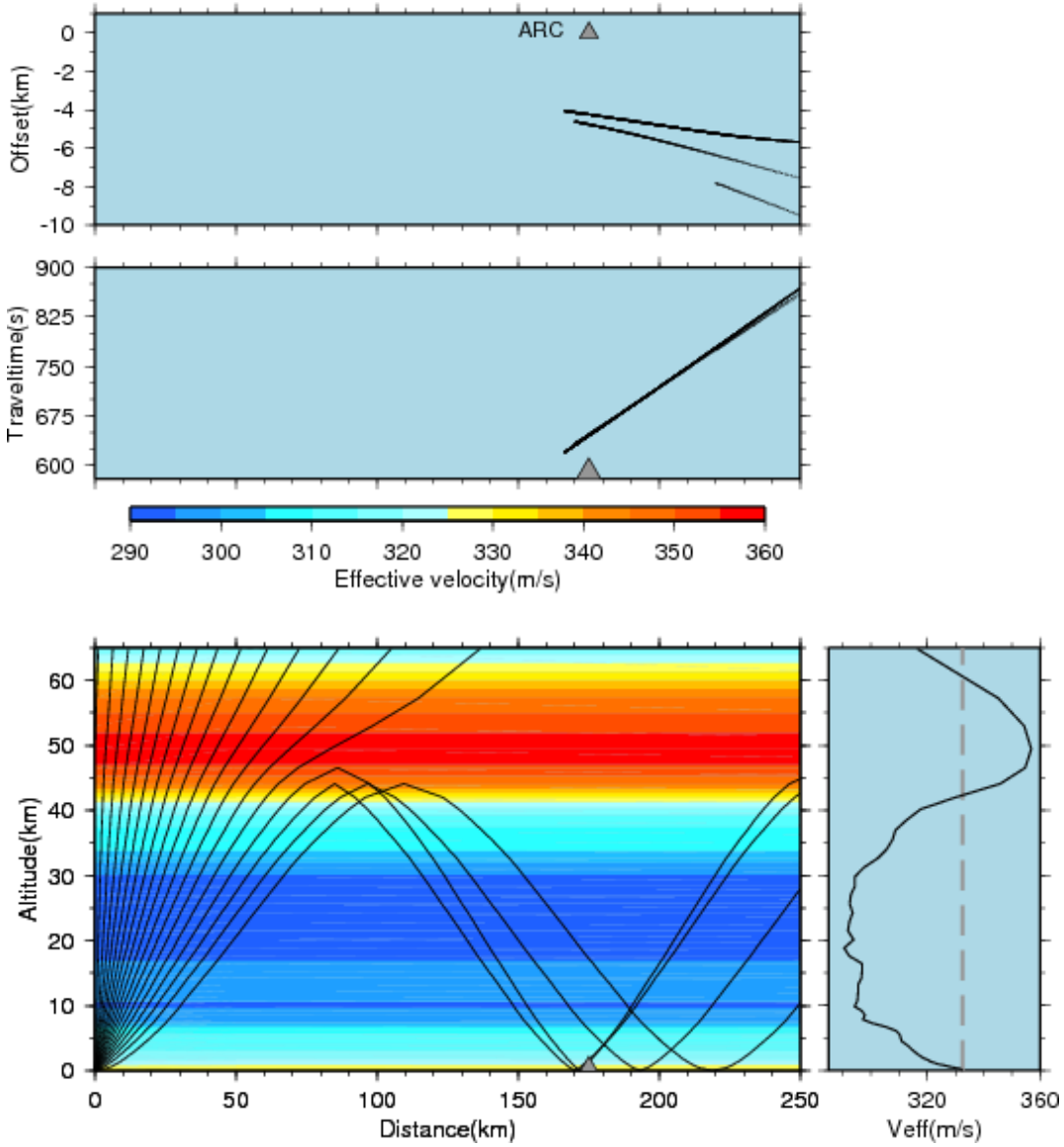

Figure 6: Raytracing results through the effective sound speed profile for energy leaving the source in the direction of ARC. The atmospheric trajectories (lower frame), traveltimes (middle frame) and offsets (upper frame) are given.

The amplitudes and directions indicate that the vortex is regaining its strength and building up towards its winter state. It follows from the above that a component of the wind field is directed from the source towards the receiver. Therefore, refractions from the stratosphere are expected as can be seen in Figure 6. Infrasound arrives at ARC from altitudes between 40 and 45 km. The average traveltime of the *Is* phases is 657 s and they occur with azimuthal deviations between -1.4 and -1.6 deg. It follows from the above examples that both tropospheric (*Iw*) and stratospheric phases (*Is*) are likely be recorded at ARC as a result from the explosions in northern Finland. *Iw* phases can be refracted from various altitudes, i.e. 500 m and 9 km in this specific

example. Traveltimes for these phases are in the order of 530 s. *Is* phases are also predicted as the polar vortex is building up to its winter state. Traveltimes for the *Is* phases are around 660 s, making traveltime a sound criterion to distinguish between *Iw* and *Is* phases. Cross winds are both strong in the troposphere and stratosphere during this specific time of the year, i.e. August and September. Therefore, azimuthal deviation is a less likely candidate for phase identification.

5. DISCUSSION

The goal of this study is to understand all infrasound recordings in ARC which occur during the build up of the polar vortex, i.e. August and September. Furthermore, the source-receiver distance of 179 km is really on the edge of the first bounce range for *Is* arrivals. The combination of both makes this a challenging task. Modeling all observed arrivals (see Figure 2) following the above approach, reveals that hardly any *Is* phases are predicted, except for the ones in 2004, September. This indicates that either that the wind and/or temperature specifications are incorrect, or that the modeling is insufficient. Both issues will be addressed in detail, resulting in the hypothesis that partial reflection on fine scale structure might be responsible for the observed *Is* phases.

REFERENCES

1. O. Dahlman, S. Mykkeltveit and H. Haak,. *Nuclear Test Ban* (Springer, Dordrecht, 2009).
2. L. G. Evers, L. Ceranna, H. W. Haak, A. Le Pichon and R. W. Whitaker, A seismoacoustic analysis of the gas-pipeline explosion near Ghislenghien in Belgium, *Bull. Seism. Soc. Am.* **97**, 417-425 (2007).
3. K. D. Koper, T. C. Wallace and R. C. Aster, Seismic recording of the Carlsbad, New Mexico, pipeline explosion on 19 August 2000, *Bull. Seism. Soc. Am.* **93**, 1427-1432 (2003).
4. A. Le Pichon, J. Guilbert, M Vallee, J. X. Dessa and M. Ulziibat, Infrasonic imaging of the Kunlun Mountains for the great 2001 China earthquake, *Geoph. Res. Lett.* **30**, 1814 (2003).
5. J. P. Mutschlecner and R. W. Whitaker}, Infrasound from earthquakes, *J. Geoph. Res.* **110**, D01108 (2005).
6. L. Ottemoller and L. G. Evers, Seismo-acoustic analysis of the Buncefield oil depot explosion in the UK, 2005, *Geoph. J. Int* **172**, 1123-1134 (2008).
7. M. H. McKenna, B. W. Stump, S. Hayek, J. R. McKenna and T. R. Stanton, Tele-infrasonic studies of hard-rock mining explosions, *J. Acoust. Soc. Am.* **122**, 97-106 (2007).
8. K. Antier, A. Le Pichon, S. Vergniolle, C. Zielinski and M. Lardy, Multiyear validation of the NRL-G2S wind fields using infrasound from Yasur, *J. Geoph. Res* **112**, D23110 (2007).
9. S. J. Gibbons, F. Ringdal and T. Kvaerna, Joint seismic-infrasonic processing of recordings from a repeating source of atmospheric explosions, *J. Acoust. Soc. Am.* **122**, EL158 (2007).
10. E. E. Gossard and W. H. Hooke, *Waves in the atmosphere* (Elsevier Scientific Publishing Company, Amsterdam, 1975).
11. J. R. Holton, *An introduction to dynamic meteorology* (Academic Press, London, 1979).
12. M. L. Salby, *Fundamentals of atmospheric physics* (Academic Press, San Diego, 1996).
13. L. C. Sutherland and H. E. Bass, Atmospheric absorption in the atmosphere up to 160 km, *J. Acoust. Soc. Am.* **115**, 1012-1032 (2004).
14. M. A. Garces, and R. A. Hansen and K. G. Lindquist, Traveltimes for infrasonic waves propagating in a stratified atmosphere, *Geoph. J. Int* **135**, 255-263 (1998).
15. A. E. Hedin and E. L. Fleming and A. H. Manson and F. J. Schmidlin and S. K. Avery and R. R. Clark and S. J. Franke, G. J. Fraser, T. Tsuda, F. Vial and R. A. Vincent, Empirical wind model for the upper, middle and lower atmosphere, *J. Atm. Terr. Phys.* **58**, 1421-1447 (1996).